3D atlas of the pituitary gland of the model fish medaka

Muhammad Rahmad Royan[1], Khadeeja Siddique[1], Gergely Csucs[2], Maja A. Puchades[2], Rasoul Nourizadeh-Lillabadi[1], Jan G. Bjaalie[2], Christiaan V. Henkel[1], Finn-Arne Weltzien[1], Romain Fontaine[1]*

[1] Physiology unit, Faculty of Veterinary Medicine, Norwegian University of Life Sciences, Ås, Norway

[2] Institute of Basic Medical Sciences, University of Oslo, Oslo, Norway

*Corresponding author: romain.fontaine@nmbu.no

Highlights:

- We offer the first 3D atlas of a teleost pituitary, which presents a valuable resource to the endocrinology and model fish community.
- The atlas reveals the 3D spatial distribution of the seven endocrine cell types and blood vessels in the juvenile/adult male and female pituitary.
- Gene expression for *tshba* and *pomca*, as well as the population size of cells expressing these genes, displays obvious sexual dimorphism in the adult medaka pituitary.
- Multi-color *in situ* hybridization and single cell RNA-seq reveal the existence of bi-hormonal cells, co-expressing *lhb-fshb*, *fshb-tshba*, *lhb-sl*, and a few multi-hormonal cells.
- An online version of the atlas is available at https://www.nmbu.no/go/mpg-atlas.

Abstract

In vertebrates, the anterior pituitary plays a crucial role in regulating several essential physiological processes via the secretion of at least seven peptide hormones by different endocrine cell types. Comparative and comprehensive knowledge of the spatial distribution of those endocrine cell types is required to better understand their role during the animal life. Using medaka as the model and several combinations of multi-color fluorescence *in situ*

hybridization, we present the first 3D atlas revealing the gland-wide distribution of seven endocrine cell populations: lactotropes, thyrotropes, Lh and Fsh gonadotropes, somatotropes, and *pomca*-expressing cells (corticotropes and melanotropes) in the anterior pituitary of a teleost fish. By combining *in situ* hybridization and immunofluorescence techniques, we deciphered the location of corticotropes and melanotropes within the *pomca*-expressing cell population. The 3D localization approach reveals sexual dimorphism of *tshba*- and *pomca*-expressing cells in the adult medaka pituitary. Finally, we show the existence of bi-hormonal cells co-expressing *lhb-fshb*, *fshb-tshba* and *lhb-sl* using single-cell transcriptomics analysis and *in situ* hybridization. This study offers a solid basis for future comparative studies of the teleost pituitary and its developmental plasticity.

Key words: *in situ* hybridization, immunofluorescence, 3D, pituitary, medaka, hormone, atlas, single cell transcriptome, teleost

Introduction

In vertebrates, the pituitary is considered the *chef d'orchestre* of the endocrine system, regulating several essential biological and physiological functions throughout the life cycle. Located beneath the hypothalamus, it is divided into the anterior part (adenohypophysis) and posterior part (neurohypophysis). The former comprises several endocrine cell types which produce and release specific peptide hormones (1, 2), controlling many important aspects of life, including growth, stress, metabolism, homeostasis, and reproduction (3).

During embryogenesis, different cellular developmental trajectories specify several endocrine cell types in the adenohypophysis, characterized by the hormones they produce (4). In general, the vertebrate adenohypophysis consists of lactotropes (producing prolactin; Prl), corticotropes (adrenocorticotropic hormone; Acth), thyrotropes (thyrotropin; Tsh), gonadotropes (follicle-stimulating and luteinizing hormone; Fsh and Lh), somatotropes (growth hormone; Gh), and melanotropes (melanocyte-stimulating hormone; α-Msh), which have specific roles in regulating certain physiological functions (2, 5). Teleosts, in addition, have an endocrine cell type that is unique to these animals, i.e. somatolactotropes (somatolactin; Sl) (6). In contrast to mammals and birds, Fsh and Lh are mostly secreted by distinct endocrine cell types in teleosts (7), although both transcripts or hormones have

sometimes been observed in the same cells in some species (8-11). Unlike mammals, teleost endocrine cells are arranged in discrete zones. Lactotropes and corticotropes are commonly located in the *rostral pars distalis* (RPD), thyrotropes, gonadotropes, and somatotropes in the *proximal pars distalis* (PPD), and melanotropes and somatolactoropes in the *pars intermedia* (PI) (6, 12).

Over the past five decades, endocrine cell type organization in the teleost pituitary has been documented in various species. Despite having approximately similar patterns, the pituitary endocrine cell maps exhibit differences in terms of variety of cell types that are reported. For instance, the localization of endocrine cell populations in dorado fish shows only four distinct types of endocrine cells across the adenohypophysis (13). By contrast, the other studies describe five (Japanese medaka (14)), six (fourspine sculpin, (15); cardinal and bloodfin tetra (16)), seven (greater weever fish, (17); white seabream, (18); dimerus cichlid (19)), and eight (Atlantic halibut, (20); Nile tilapia, (21); saddle wrasse, (22)) cell types.

Even though these previous studies have provided interesting information on the spatial organization of endocrine cell populations, they lack information due to the techniques available and used at the time. First, the use of mid- and para-sagittal sections of the pituitary to reconstruct organizational patterns of endocrine cells leads to a lack of information on the lateral sides. Second, the single-labeling method and non-species specific antibodies that are typically used do not provide sufficient detail on arrangements among adjacent endocrine cell populations, or on the possible existence of multi-hormonal cells as described in mammals (23-26). These features will be important to better understand the underlying processes in fish physiology and endocrinology. Moreover, the distribution of the blood vessels within the pituitary, which play an essential role by transporting the released hormones, is poorly known. A better knowledge will help understand how endocrine cells arranged within a vascularized system that is thought to facilitate paracrine signaling in the pituitary (27). Also, since it has been shown that the pituitary is a plastic organ with changes occurring at cellular and population levels (28), it is essential to describe the cell composition, spatial organization, and vascularization of the pituitary in detail.

The Japanese medaka (*Oryzias latipes*) is a teleost model commonly used to investigate vertebrate and teleost physiology, genetics, and development, due to easy access to a wide range of genetic and molecular techniques (29, 30). We have recently used single-cell RNA sequencing to describe seven distinct endocrine cell types (expressing *prl*, *pomca*, *fshb*, *lhb*,

tshba, *gh*, and *sl*) in the medaka pituitary (31). Here, we extend this study by describing differences present in the spatial distribution of the seven endocrine cell populations, in juvenile and adult fish from both sexes. Using multi-color *in situ* hybridization techniques together with single-cell transcriptomics analysis, this study offers the first 3D atlas of teleost pituitary endocrine cell populations, allowing the identification of differences in spatial distribution patterns between sexes and stages, as well as the existence of multi-hormonal cells.

Materials and Methods

Experimental animals

Juvenile (2-month old) and adult (6-month old) wild type medaka (WT, d-rR strain) were reared at 28 ºC in a re-circulating water system (pH 7.5; 800 µS) with 14 hours light and 10 hours dark conditions. Fish were fed three times daily using artemia and artificial feed. Sex determination was based on secondary sexual characteristics (32). Experiments were conducted in accordance with recommendations on experimental animal welfare at the Norwegian University of Life Sciences.

Quantitative Polymerase Chain Reaction (qPCR)

RNA extraction from pituitaries (n = 7) was performed as previously described in (33). Fish were euthanized by immersion in ice water and pituitaries were collected and stored at -80 ºC in 300 µl of TRIzol® (Invitrogen, Carlsbad, USA) with 6 zirconium oxide beads (Bertin Technologies, Versailles, France; diameter 1.4 µm). Later, tissues were homogenized and mixed with 120 µl chloroform. The pellet was reconstituted with 14 µl of nuclease free water. Due to the size of the tissue, 3 juvenile pituitaries were pooled to represent one replicate of each sample. A total of 33 ng of RNA was used to synthesize cDNA using SuperScript III Reverse Transcriptase (Invitrogen, Carlsbad, CA, USA) and random hexamer primers (Thermofisher scientific). 5× diluted cDNA samples were analyzed in duplicate, using 3 µL of the cDNA and 5 µM each of forward and reverse primer in a total volume of 10 µL (**Table 1**). The parameter cycle was 10 min pre-incubation at 95 °C, followed by 42 cycles of 95 °C for 10 s, 60 °C for 10 s and 72 °C for 6 s, followed by melting curve analysis to assess PCR product specificity. The mRNA level was normalized using

rpl7 as reference gene as it was found no significant difference of expression between groups.

Multi-color fluorescence *in situ* hybridization (Multi-color FISH)

Tissue preparation: Fish were euthanized by immersion in ice water. Brain and pituitary were taken and fixated overnight at 4 ºC in 4% paraformaldehyde (PFA, Electron Microscopy Sciences, Hatfield, Pennsylvania) diluted with phosphate buffered saline with Tween (PBST: PBS, 0.1%; Tween-20), approximately 50× the tissue volume. Tissue was then dehydrated using a series of increasing ethanol concentrations: 25%, 50%, 75%, 96% followed by a storage in 100% methanol at -20 ºC until use.

Cloning and RNA probe synthesis: DNA sequences for the probes were obtained from NCBI as listed in **Table 2**. Sequences are selected according to the high expression in the pituitary for those having more than one paralog in the medaka genome (*tshb* and *pomc*). PCR primers for the amplification of the probe genes were designed from transcribed sequences (mRNA) for each gene using Primer3 (https://primer3.ut.ee/). Following RNA extraction and cDNA synthesis as described above, cDNA was used to amplify the sequence of interest by PCR using Taq DNA polymerase (Thermo Fisher Scientific) with a 3-min denaturation step at 94 ºC, followed by 35 cycles at 94 ºC for 15s, 50 ºC for 15s, and 72 ºC for 60s, and finally 1 cycle of 72 ºC for 5 mins. The amplified PCR products were isolated using a gel extraction kit (Qiagen) and cloned into the pGEM-T Easy vector (Promega) following manufacturer instructions and verified by sequencing. PCR products from the verified plasmids were used as template to synthetize sense and anti-sense complementary RNA probes using *in vitro* transcription with T7 or SP6 RNA polymerase (Promega, Madison, Wisconsin). RNA probes were tagged with dinitrophenol-11-UTP (DNP, Perkin Elmer, Waltham, Massachusetts), fluorescein-12-UTP (FITC, Roche Diagnostics), or digoxigenin-11-UTP (DIG, Roche Diagnostics). Finally, the probes were purified using the Nucleospin RNA clean-up kit (Macherey-Nagel, Hoerdt, France) and the concentration was measured using the Epoch Spectrophotometer System (BioTek, Winooski, VT, USA).

Multi-color fluorescence *in situ* hybridization (FISH): Multi-color FISH was performed as previously described in (34) with minor modifications. Tissues were serially rehydrated, and the pituitary was detached from the brain. Afterwards, whole pituitaries were hybridized with the probes (0.11 – 3.17 ng/µl) for 18 hours at 55 ºC, and incubated with different

combinations of anti-DNP- (Perkin Elmer), anti-FITC-, and anti-DIG-conjugated antibodies (Roche Diagnostics), followed by TAMRA- (Thermofisher), Cy5- (Perkin Elmer) and FITC-conjugated tyramides (Sigma). The nuclei were stained with DAPI (1:1000, 4', 6-diamidino-2-phenylindole dihydrochloride; Sigma). The absence of labeling when using sense probes was used to confirm the specificity of the anti-sense probes. Whole pituitaries were mounted using Vectashield H-1000 Mounting Medium (Vector, Eurobio/Abcys) between microscope slides and cover slips (Menzel Glässer, VWR) with spacers (Reinforcement rings, Herma) in between for the juveniles, and between two cover slips with spacers for adults.

Combined FISH and Immunofluorescence (IF)

To distinguish the localization of adrenocorticotropic releasing hormone (Acth) and alpha-melanocyte stimulating hormone (α-Msh) cells within *pomca*-expressing cells separately, IF was performed using the antibodies shown in **Table 3**. After FISH for *pomca* labelled with FITC-conjugated tyramide, the pituitaries were embedded in 3% agarose (H_2O) and para-sagittally sectioned with 60 µm thickness using a vibratome (Leica). From a single pituitary, odd and even ordered slices were processed to detect Acth and α-Msh IF, respectively. Tissue slices were incubated for 10 minutes at room temperature (RT) in permeabilizing buffer (0.3 % Triton in PBST) with agitation, before incubation for 1 hour at RT in blocking solution (Acth: 3% normal goat serum (NGS); 0.3% Triton; 1% dimethylsulfoxide (DMSO) in PBST; α-Msh: 3% NGS; 5% Triton; 7% DMSO in PBST). Sections were then incubated at 4 °C overnight with primary antibodies (diluted in blocking) or without (control), followed by 4 hours at RT with secondary antibodies (diluted in blocking) with extensive PBST washes in between. Nuclei were stained with DAPI (1/1000). Controls were performed as described above incubating the tissue without the primary antibodies and confirming the absence of fluorescent signals. The antibody dilution is provided in **Table 3**.

Blood vessel staining

Blood vessels were stained by cardiac perfusion as previously described in (35). The fish were anesthetized with 0.04% Tricaine (pH 7), and the anterior abdomen was cut to let the heart opening adequately wide for the injection. Afterwards, 0.05% of DiI (1,1'-Dioctadecyl-3,3,3',3'-Tetramethylindocarbocyanine Perchlorate; Invitrogen) solution diluted in 4% PFA (in PBS) was administered to the *bulbus arteriosus* through the ventricle using a glass

needle. The pituitary was dissected and fixated in 4% PFA (in PBS) for 2 hours in the dark before being washed 2 times with PBS and mounted as described above.

Image processing and analysis

Fluorescent images were obtained using an LSM710 Confocal Microscope (Zeiss, Leica) with 25× (for adult pituitary) and 40× (for juvenile pituitary) objectives. Filters with wavelength of 405 (DAPI), 555 (TAMRA; Alexa-555), 633 (Cy5) and 488 (FITC; Alexa-488) nm were used. Due to the size of the adult pituitaries, the image acquisition was done from the dorsal and ventral sides of the pituitary with some overlaps in the middle. In conjunction with the microscope, ZEN software (v2009, Zeiss) was used to process the images, and ImageJ (1.52p; http://rsbweb.nih.gov/ij/) was used for processing z-projections from confocal image stacks. The dorsal and ventral stacks of adult pituitaries were aligned using HWada (https://signaling.riken.jp/en/en-tools/imagej/635/) and StackReg plugin (http://bigwww.epfl.ch/thevenaz/stackreg/), before presenting them in orthogonal views.

3D atlasing

While juvenile pituitaries were imaged as one block, adult pituitaries were imaged from the ventral and dorsal side with confocal imaging as described above. The two sides of the adult pituitaries were then merged using landmarks as visible with the DAPI staining. Finally, eight pituitaries labeled for different markers were aligned to the same coordinate system also using manually selected landmarks. These data were used for the creation of four 3D atlases of the pituitary gland, using the principle approaches outlined in (36).

The creation of the 3D atlases involved several steps. Merging and alignment was done using LandmarkReg (https://github.com/Tevemadar/LandmarkReg, with accompanying utilities https://github.com/Tevemadar/LandmarkReg-utils). Image stacks were saved in NIfTI format (https://imagej.nih.gov/ij/plugins/nifti.html) and converted with the "NIfTI2TopCubes" utility before the matching anatomical positions ("landmarks") were manually identified in volume-pairs. Both the signal from endocrine cells and the DAPI background were inspected, and four or more landmarks were recorded for each volume-pair. In case of ventral-dorsal half images (adult samples), a custom utility "PituBuild" was used for merging the two halves, based on partial overlap. Finally, each set of complete pituitary volumes was aligned to a common anatomical space using the "Match" utility. The resulting NIfTI volumes were then converted to TIFF stacks for viewing and analysis.

To enable 3D viewing of the pituitary atlases, data were prepared for the MeshView tool (RRID:SCR_017222, https://www.nitrc.org/projects/meshview/) developed for 3D brain atlas viewing (37). Volumes were first binarized using the "BinX" utility with a threshold value of 50. MeshGen (https://www.nitrc.org/projects/meshgen/) was then used to generate surface meshes in standard STL format (http://paulbourke.net/dataformats/stl/) before convertion using PackSTL (https://github.com/Tevemadar/MeshView-PackSTL) to allow viewing in MeshView.

Single cell transcriptomics analysis (scRNA-seq)

We used processed scRNA-seq dataset for male and female pituitaries (31) and filtered out red blood cells to avoid noise. Next, we applied a cut-off to differentiate between cells with high and low expression for specific genes (Supp. Fig. 1). This dataset is further used to generate the pair-wise scatterplots using the R package ggplot2 (version 2_3.3.2), to show cells expressing more than one hormone-producing gene. Finally, we got 191 and 229 multiple hormone-producing cells in female and male pituitaries, respectively. We generated clustered heatmaps using pheatmap (version 1.0.12) to visualize the expression levels of hormone-producing genes in each cell expressing multiple hormones.

Statistical analysis

Levene's test was performed to analyze the homogeneity of variance while the normality was tested using the Saphiro-Wilk Normality test. The differences in mRNA levels were evaluated using One-way ANOVA followed by Tukey *post hoc* test. The data are shown as mean + SEM (Standard Error of Mean) unless otherwise stated in the figure legend. $p < 0.05$ was used as a threshold for statistical significance.

Data availability

All image files are available in a data repository (link coming soon). The 3D atlases (Fig. 1) can be found on a webpage containing explanatory videos and other types of data completing the online pituitary atlas (https://www.nmbu.no/go/mpg-atlas), allowing easy access and navigation through the data.

Results

3D atlases of the medaka pituitary

Using several combinations of multi-color FISH, we combined the labeling to form four 3D pituitary atlases now available online (http://meshview.uiocloud.no/Medaka-pituitary/?JF; http://meshview.uiocloud.no/Medaka-pituitary/?JM; http://meshview.uiocloud.no/Medaka-pituitary/?AF; http://meshview.uiocloud.no/Medaka-pituitary/?AM), allowing us to precisely localize the seven endocrine cell types (*prl*, *pomca*, *tshba*, *fshb*, *lhb*, *gh* and *sl*) in the adenohypophysis of medaka.

1. *prl*-expressing cells (lactotropes)

In both adults and juveniles (Supp. Fig. 2), *prl*-expressing cells make up almost the entirety of the RPD from the dorsal to the ventral side of the pituitary, without any obvious difference in localization pattern between males and females. They border on and intermingle with a *pomca*-expressing cell population (Supp. Fig. 9). In some fish, a few *prl*-expressing cells are also localized peripherally in the dorsal area of PPD (data not shown).

2. *pomca*-expressing cells (corticotropes and melanotropes)

pomca-expressing cells are observed in two distinct places in the pituitary. One population is localized in the dorsal part of RPD, where it is mostly clustered in the middle if observed from transverse point of view, and the second is detected in the PI area (Supp. Fig. 3). While the first one is adjacent to and mixing with *prl*-expressing cells, in close proximity to *tshba*-expressing cells (Supp. Fig. 9), the second population intermingles with *sl*-expressing cells (Supp. Fig. 10).

3. *tshba*-expressing cells (thyrotropes)

tshba-expressing cells are localized in the dorsal side of anterior PPD towards the PN, next to the *prl*- and *pomca*-expressing cells (Supp. Fig. 4 and Supp. Fig. 9). From a transverse point of view, *tshb*-expressing cells are mostly concentrated in the middle part of the PPD (Supp. Fig. 4) where they border and mix with *fshb*-expressing cells (Supp. Fig. 11).

4. *fshb*-expressing cells (gonadotropes)

fshb-expressing cells are detected from the anterior to middle part of the PPD, distributed in both lateral sides of the pituitary from a transverse point of view (Supp. Fig. 5). These cells

cover the PN from a frontal point of view (Supp. Fig. 5). They border and mix with *tshba*-expressing cells in the dorsal (Supp. Fig. 11), *lhb*-expressing cells in the ventral (Supp. Fig. 12) and *gh*-expressing cells in the posterior part of the PPD (Supp. Fig. 13).

5. *lhb*-expressing cells (gonadotropes)

In both juveniles and adults, *lhb*-expressing cells are commonly distributed in the peripheral area of the PPD, covering almost the entire ventral side of the pituitary (Supp. Fig. 6). In adults, *lhb*-expressing cells are also localized in the proximity of peripheral area of the PI (Supp. Fig. 6). These cells border and mix with *fshb*-expressing cells in the PPD (Supp. Fig. 12), and with *pomca*- and *sl*-expressing cells in the PI of adult pituitary (Supp. Fig. 10).

6. *gh*-expressing cells (somatotropes)

gh-expressing cells are localized on the dorsal side of the PPD towards the PN area (Supp. Fig. 7). Similar to *fshb*-expressing cells, which are distributed to both lateral sides of the pituitary, *gh*-expressing cells are more towards the posterior part of the PPD, encompassing and bordering with the PN (Supp. Fig. 7), mixing with *fshb*-expressing cells (Supp. Fig. 13).

7. *sl*-expressing cells (somatolactotropes)

sl-expressing cells are intermingled within *pomca*-expressing cells located in the PI (Supp. Fig. 8 and Supp. Fig. 10). In the adult pituitary, these cells border and mix with *lhb*-expressing cells that are detected in the proximity of the PI (Supp. Fig. 10).

8. Distinction of Acth and α-Msh cell populations

The combination of FISH for *pomca* with IF for Acth or α-Msh shows that that Acth cells overlap the entire *pomca* signal, while melanotropes overlap *pomca* signals that are located in the PI, both in adults (Fig. 2) and in juvenile pituitaries (Supp. Fig. 14).

9. Blood vessels

3D reconstruction shows that blood vessels encompass the entire adenohypophysis, without any obvious difference observed between sexes and stages (Fig. 3).

Sex and stage differences

FISH and qPCR data did not reveal any difference in *prl*- and *gh*-expressing cell number or mRNA levels between sexes and stages. In contrast, adult females show significantly higher mRNA levels in both *fshb* ($p < 0.01$) and *lhb* ($p < 0.0001$) compared to the other groups, while *lhb* mRNA levels are significantly higher in adult males than in juveniles ($p < 0.05$) (Fig. 4), despite no obvious difference in the cell population size (Supp. Fig. 4-5). *sl* mRNA levels are significantly higher in juveniles compared to adult males ($p < 0.05$) (Fig. 4) without any obvious difference in cell number (Supp. Fig. 8).

In contrast, FISH revealed that the population of *tshba*-expressing cells is larger in adult females, expanding from the anterior to the middle part of PPD, whereas in adult males and juveniles they are found only in the anterior part of the PPD (Supp. Fig. 4). This agrees with the significantly higher *tshba* mRNA levels observed by qPCR in the adult female group compared to the other groups ($p < 0.0001$) (Fig. 4). The *tshba*-expressing cell population also appears larger in juveniles than in adult males using FISH, in line with significantly higher level of *tshba* mRNA observed by qPCR in juveniles compared to in adult males ($p < 0.05$) (Fig. 4 and Supp. Fig. 4).

pomca mRNA levels in adult male are significantly higher than the other groups ($p < 0.0001$), and this agrees with the *pomca*-expressing cell population illustrated in Fig. 2, Supp. Fig. 3 and Supp. Fig. 14, where there are bigger populations of *pomca* cells in adult male than the other groups.

Despite obvious differences in mRNA transcript levels and cell number observed with qPCR and FISH/IF labeling, we could not observe any difference in the proportion of each cell type between males and females with the scRNA-seq data.

Cells producing multiple hormones

Using scRNA-seq data, we observed some bi-hormonal cells in the pituitary of adult medaka (Fig. 5). Both sexes show a number of cells co-expressing *lhb*- and *fshb*-, *lhb*- and *tshba*- and *fshb* and *tshba*. Meanwhile, some cells co-expressing *lhb* and *sl*, *fshb* and *sl*, *fshb* and *prl*, *fshb* and *pomca*, *tshba* and *prl*, *tshba* and *pomca*, *prl* and *gh*, and *prl* and *pomca* are unique to adult males, whereas co-expression of *fshb*- and *gh*-expressing cells is only found in adult females (Fig. 5A). The co-expression between *lhb-fshb* and *fshb-tshba* in both sexes and *lhb-sl* in adult male was confirmed using multi-color FISH (Fig. 6). While the co-

354 localization of cells expressing *lhb-fshb* and *fshb-tshba* was observed in several individuals,
355 the *lhb-sl* expressing cells were observed only in 1 out of 13 adult male pituitaries analyzed.

356 Several cells also co-express more than two hormone-encoding genes, although these are
357 rare compared with bi-hormonal cells (Fig. 5B), and in this study they could not be
358 confirmed using multi-color FISH.

359

360 Discussion

361 3D spatial distribution of endocrine cell populations and blood vessels

362 We have recently used scRNA-seq to identify and characterize seven endocrine cell types
363 in the teleost model organism medaka (31). Although a 3D atlas of the pituitary gland
364 development has been previously described in zebrafish (38), the present atlas is the first 3D
365 atlas of all pituitary endocrine cell populations in a teleost fish. It provides more precise and
366 detailed information on the distribution and organization of the different cell types, and
367 clearly demonstrate that endocrine cells are distributed differently when comparing mid-
368 sagittal with para-sagittal sections (Fig. 7).

369 As reported in coho (39) and chum salmon (40, 41), seabass (42), gilt-head seabream (43),
370 common barbel (44) and striped bass (45), we observed some lactotropes in the ventro-
371 peripheral area of the PPD. However, these cells were found only in some fish and not
372 always at the same location, which makes them difficult to map. We found Lh gonadotropes
373 in the PI, in addition to in the PPD, but only in adults, and we did not observe Lh cells in
374 RPD as reported by some studies (16, 17, 46-48). The extra-PPD localization of Lh
375 gonadotropes might be due to PPD extension (20) or Lh cell migration to other zones during
376 the ontogeny of the adenohypophysis (49). Meanwhile, several studies reported
377 somatotropes in the RPD (45, 50) and PI (51, 52), and somatolactotropes and melanotropes
378 in the PPD (13, 16-18, 51). However, we did not observe this in medaka. The wide
379 localization of Gh, Sl, and α-Msh cells in these studies might also be explained by antigenic
380 similarities as suggested in (13, 16, 53).

381 The blood vasculature is ubiquitously spread over almost the entire adenohypophysis in
382 medaka, without obvious differences between sexes and stages. This agrees with previous
383 studies in zebrafish (54, 55) showing a highly vascularized pituitary. Such complex
384 vasculature is, of course, central to the endocrinological function of the pituitary, as it allows

for the efficient transport of secreted hormones to peripheral organs. In addition, it may facilitate intra-pituitary paracrine signaling (27).

Sexual dimorphism of *tshba*- and *pomca*-expressing cell populations

While it seems impossible to show differences of endocrine cell population between sexes and stages when the data only rely on para-sagittal sections of the pituitary, whole pituitary labeling methods allow their identification. For instance, we show for the first time that *tshba*- and *pomca*-expressing cell populations are more numerous in adult females and males, respectively. Our qPCR data on *tshba* and *pomca* levels agree with previous studies in medaka (56) and further support the sexual dimorphism. In the previous medaka study, androgens were suggested to be involved in *tshb* suppression in adult males via activation of *tph1* transcription expressed in *pomc*-expressing cells. This is important for serotonin synthesis, which plays a role in repressing the expression of some endocrine cell markers, including *tshb*. We also found significantly lower *tshba* levels in adult compared to in juvenile males where the androgen levels are generally lower (for review, see (57, 58)), supporting the inhibitory role of androgens on *tshba* levels. It will be interesting to challenge this hypothesis in future research using orchidectomy which allows for androgen clearance in the medaka (59). However, although higher *tshb* levels are also observed in female half-barred wrasse (60) and *tshb* levels are higher in juvenile than in adult male Atlantic salmon (61), zebrafish shows no sexual dimorphism of *tshb* and *pomc* (62), suggesting species differences.

We also observed sexual dimorphism of *fshb* and *lhb* mRNA levels in adults, in agreement with a previous medaka study (56). This suggests a difference in gonadotrope cell activity as we did not observe a difference in population size, also supported by the absence of significant differences in Lh or Fsh cell numbers in previous studies (9, 63). In contrast, we observed an increase of *lhb* mRNA levels between juvenile and adult stages, which might mainly be due to an increase in cell numbers as shown in (63). Surprisingly, we did not observe a significant difference in *fshb* mRNA levels between juveniles and adults, while an increase in Fsh cell numbers has also been reported during sexual maturation (9). While neither sexual dimorphism nor stage differences were observed in *prl* or *gh* levels, we found stage difference in *sl* levels, with higher levels in juveniles than in adults. Somatolactin has been associated with sexual maturation in some teleosts, such as coho salmon (64), Nile tilapia (65) and flathead grey mullet (66). The upregulation of *sl* levels in teleosts is thought

418 to be related to gonadal growth, as it is highly expressed at the onset of gonadal growth and
419 lowly expressed post-ovulation (67, 68). This implies that in the current study, the adult fish
420 used might be in a post-ovulation phase while the juveniles appear to enter gonadal
421 development.
422

423 **scRNA-seq and multi-color FISH reveal the presence of multi-hormonal cells**
424 **in the adult medaka pituitary**

425 The presence of cells expressing more than one hormone in the anterior pituitary has been
426 shown in many studies, both in teleosts and in mammals (for review see (28, 69-71)). Using
427 scRNA-seq technology, multi-hormonal cells have for instance been described in the mouse
428 pituitary (72). However, using similar approaches, pituitary multi-hormonal cells have not
429 been reported in teleosts (31, 73), although some studies have documented cells producing
430 more than one hormone in the teleost pituitary (8-11).

431 Here, we show the presence of gonadotrope cells expressing both *lhb* and *fshb* which has
432 previously been reported in medaka (9) and in other teleost species (8, 10, 11). One proposed
433 underlying mechanism that could explain the existence of such bi-hormonal gonadotropes
434 is their capacity to change phenotype, with a transitory bi-hormonal state as suggested by *in*
435 *vitro* observation where Lh cells were found to become Fsh (9). We also found cells co-
436 expressing *fshb-tshba* and *sl-lhb*. Although previous immunohistochemtry studies on the
437 pituitary of several teleost species showed cross-reaction between Tsh and Lh/Fsh (43, 53)
438 and between Lh and Sl antibodies (16, 53, 74, 75), we show specific labeling of *tshb*, *fshb*,
439 *lhb*, and *sl* in the current study confirming the specificity of the probes. Therefore, the
440 observation of colocalization of *fshb-tshba* and *sl-lhb* supports that these bi-hormonal cells
441 exist in the medaka pituitary. Meanwhile, a number of studies have shown co-staining
442 between Prl, Gh and Sl (13, 20, 22, 40, 51). However, our scRNA-seq data exhibit only a
443 few cells co-expressing *prl* and *gh*. While antigenic similarities could be the reason of co-
444 staining between these cell types (13, 16, 53), their low occurrence in the medaka pituitary
445 might be the reason of being unable to observe them with FISH.

446 Within the *pomca*-expressing cell population, we observed Acth staining alone at the border
447 of the RPD/PPD and staining of both Acth and α-Msh in the PI. Co-staining between Acth
448 and α-Msh is not uncommon as Acth-immunoreactive cells have been found in RPD and PI
449 areas in other teleost species (8, 18, 20-22, 42, 43, 76). However, it must be noted that the
450 target antigen of anti-Acth used in this study and most previous studies contains the target

antigen for anti-α-Msh (https://www.uniprot.org/uniprot/P01189#PRO_0000024970). This might explain why we found both Acth and α-Msh cells in the PI. A previous study pre-incubating anti-Acth with α-Msh antigen demonstrated that Acth cells are localized in the RPD while α-Msh cells are found in the PI (21). This might also be the case in medaka.

We also show that a few cells in the adult medaka pituitary express more than two hormone-encoding genes. Despite having been reported in mammals (72), the current study is the first to show the presence of such multi-hormonal cells in the teleost pituitary. Although we could not confirm their existence using FISH, most likely because of the low number of such cells present in the pituitary, the demonstration of their existence using scRNA-seq raises questions about their origin and roles in the medaka pituitary.

Finally, the 3D atlas platform that is provided online will help research community to take a close look on the spatial distribution of endocrine cells and the vascularization of blood vessels in the pituitary.

Author Contributions

RF and FAW conceptualized and planned the work. RF, MAP, JB and FAW obtained funding. NR did all cloning. MRR and RF performed the experiments and acquired the imaging data. MRR and GC processed the imaging data and developed the online 3D model, supervised by MAP and JB. CH and KS analyzed the single cell transcriptome data. MRR, CH and RF wrote the paper with the inputs from all authors.

Funding

This study was funded by the Norwegian University of Life Sciences (to RF) and the Norwegian Research Council grants No. 251307, 255601, and 248828 (to FAW). The tools development received support from the European Union's Horizon 2020 Framework Programme for Research and Innovation under the Specific Grant Agreement No. 945539 (Human Brain Project SGA3) (to JGB) and the Research Council of Norway under Grant Agreement No. 269774 (INCF Norwegian Node) (to JGB).

479

480 **Conflict of Interest**

481 The authors declare that the research was conducted in the absence of any commercial or
482 financial relationships that could be construed as a potential conflict of interest.

483

484 **Acknowledgments**

485 The authors thank Ms Lourdes Carreon G. Tan for her assistance in the fish husbandry.

486

487 Figure Legends

488 **Figure 1.** 3D reconstruction of medaka anterior pituitary containing seven endocrine cell
489 populations. Illustration of brain and pituitary (pointed by black arrow) of medaka from
490 lateral view (A) and ventral view (B) (Figure is adopted and modified with permission from
491 (63)). The navigation platform of 3D spatial distribution endocrine cell population that are
492 now available online (C). Snapshots of 3D reconstruction of endocrine cell population from
493 juvenile and adult medaka male and female (D). The snapshots were captured from different
494 perspectives: free viewpoint (i), lateral (ii and iii), dorsal (iv) and ventral (iv). Four direction
495 arrows display the direction of the pituitary (A: anterior; P: posterior; D: dorsal; V: ventral).
496 The color legend shows the color code for each cell type.

497 **Figure 2.** The combination of FISH for *pomca* and IF for Acth or α-Msh allows the
498 distinction of two clear *pomca* expressing cell populations. The distinction of Acth (green)
499 and α-Msh (blue) producing cells from *pomca*-labelled (red) in the pituitary from adult male
500 and female medaka. Dashed line represents the pituitary as shown in the right panel. Four
501 direction arrows display the direction of the pituitary (A: anterior; P: posterior; D: dorsal;
502 V: ventral).

503 **Figure 3.** 3D projection of blood vessels from juvenile and adult male and female medaka
504 pituitary from the dorsal side. Left right arrow symbol shows the direction of the pituitary
505 (A: anterior; P: posterior).

506 **Figure 4.** Relative mRNA levels of endocrine cell markers (*prl*, *tshba*, *fshb*, *lhb*, *gh*, *sl* and
507 *pomca*) in juvenile and adult medaka males and females (juvenile male, JM; juvenile female,
508 JF; adult male, AM; adult female, AF). Graphs are provided as mean + SEM, and jitter dots

represent N. Different letters display statistical differences ($p < 0.05$) between groups as evaluated by One-way ANOVA followed by Tukey *post hoc* test.

Figure 5. scRNA-seq data reveal the presence of bi-hormonal and multi-hormonal cells in the medaka pituitary. Pair wise plots of 2228 cells in female and 3245 cells in male pituitary (A). Colored by filtered cells (gray), *lhb* expressing cells (green), *fshb* expressing cells (darkolivegreen), *tshba* expressing cells (cyan), *sl* expressing cells (red), *prl* expressing cells (blue), *gh* expressing cells (magenta), *pomca* expressing cells (darkgrey) and cells expressing more than one endocrine gene (purple). Light grey cells represent the cells where gene expression for the investigated hormone is considered as part of the background. Axes are log normalized. Heatmap of seven hormone-encoding genes of the female and male pituitary (B). Each row represents one cell, and left side indicates cell clustering. Low expressions are shown in blue and high expressions are shown in red. Color bars on the left indicates how different cell types clustered on the basis of expression in each cell. Black arrows show cells that strongly express more than two hormone-encoding genes.

Figure 6. Multi-color FISH reveals some cells co-expressing more than one hormone-encoding genes in the medaka pituitary. Confocal plane confirming colocalization of *lhb* and *fshb* labelings (A), and *fshb* and *tshb* (B) labelings in both male and female adult medaka pituitary. Confocal plane showing the colocalization of *lhb* and *sl* in adult male (C). White arrows show cells whose mRNAs are co-expressed, while yellow arrows show cells that do not (can be used as control of probe´s specificity). The location of the bi-hormonal cells is in the proximity of red rectangle as illustrated in the schematic drawing of pituitary in left panels.

Figure 7. Schematic illustration showing differences in distribution of endocrine cell population between mid-sagittal and para-sagittal section of the medaka pituitary. The schemas are drawn based on mid- (A) and para-sagittal (B) point of view. C) Transverse view of medaka pituitary showing approximate location of mid-sagittal (red) and para-sagittal sections (green). Four direction arrows display the direction of the pituitary (A: anterior; P: posterior; D: dorsal; V: ventral).

Supp. Fig. 1. Density plots of hormone-encoding genes in the pituitary of adult male (A) and female (B) medaka. Red line represents a cut-off to differentiate between the cells with high gene expression (considered as endocrine cells) and low gene expression (considered as background and non-endocrine cells).

Supp. Fig. 2-8. Orthogonal view of each endocrine cell types in juvenile and adult male and female medaka. (2, *prl*; 3, *pomca*; 4, *tshba*; 5, *fshb*; 6, *lhb*; 7, *gh*; 8, *sl*). The pictures were captured from different perspectives: transverse (i), frontal (ii) and para-sagittal (iii). Up down arrow symbol shows the direction of the pituitary (A: anterior; P: posterior; D: dorsal; V: ventral).

Supp. Fig. 9-13. Transverse views of multi-color FISH of endocrine cells in juvenile and adult male and female medaka. (9, *prl-tshba-pomca*; 10, *sl-lhb-pomca*; 11, *fshb-tshba*; 12, *fshb-lhb*; 13, *fshb-gh*) (A: anterior; P: posterior; D: dorsal; V: ventral).

Supp. Fig. 14. The combination of FISH for *pomca* and IF for Acth or α-Msh allows the distinction of two clear *pomca* expressing cell populations. The distinction of Acth (green) and α-Msh (blue) producing cells from *pomca*-labelled (red) in the pituitary from juvenile male and female medaka. Dashed line represents the pituitary as shown in the right panel. Four direction arrows display the direction of the pituitary (A: anterior; P: posterior; D: dorsal; V: ventral).

Table 1. Primer sequences used for the mRNA level analysis in the medaka pituitary.

Table 2. Primer sequences used to make the *in situ* hybridization (ISH) probes of seven endocrine cell types in the medaka pituitary.

Table 3. Primary and secondary antibodies used for immunofluorescence (IF) to distinguish Acth and α-Msh cells from *pomca*-expressing cells in the medaka pituitary.

References

1. Yeung C-M, Chan C-B, Leung P-S, Cheng CHK. Cells of the anterior pituitary. The International Journal of Biochemistry & Cell Biology. 2006;38(9):1441-9.
2. Ooi GT, Tawadros N, Escalona RM. Pituitary cell lines and their endocrine applications. Molecular and Cellular Endocrinology. 2004;228(1):1-21.
3. Melmed S. The pituitary: Academic press; 2010.
4. Brinkmeier ML, Davis SW, Carninci P, MacDonald JW, Kawai J, Ghosh D, et al. Discovery of transcriptional regulators and signaling pathways in the developing pituitary gland by bioinformatic and genomic approaches. Genomics. 2009;93(5):449-60.
5. Le Tissier PR, Hodson DJ, Lafont C, Fontanaud P, Schaeffer M, Mollard P. Anterior pituitary cell networks. Frontiers in Neuroendocrinology. 2012;33(3):252-66.
6. Kaneko T. Cell Biology of Somatolactin. In: Jeon KW, editor. International Review of Cytology. 169: Academic Press; 1996. p. 1-24.

574 7. Weltzien F-A, Hildahl J, Hodne K, Okubo K, Haug TM. Embryonic development of
575 gonadotrope cells and gonadotropic hormones – Lessons from model fish. Molecular and Cellular
576 Endocrinology. 2014;385(1):18-27.
577 8. Hernández MPGa, García Ayala A, Zandbergen MA, Agulleiro B. Investigation into the
578 duality of gonadotropic cells of Mediterranean yellowtail (Seriola dumerilii, Risso 1810):
579 immunocytochemical and ultrastructural studies. General and Comparative Endocrinology.
580 2002;128(1):25-35.
581 9. Fontaine R, Ager-Wick E, Hodne K, Weltzien F-A. Plasticity in medaka gonadotropes via
582 cell proliferation and phenotypic conversion. Journal of Endocrinology. 2020;245(1):21.
583 10. Candelma M, Fontaine R, Colella S, Santojanni A, Weltzien F-A, Carnevali O. Gonadotropin
584 characterization, localization and expression in the European hake (Merluccius merluccius).
585 Reproduction. 2017;153(2):123.
586 11. Golan M, Biran J, Levavi-Sivan B. A Novel Model for Development, Organization, and
587 Function of Gonadotropes in Fish Pituitary. Frontiers in Endocrinology. 2014;5(182).
588 12. Schreibman MP, Leatherland JF, McKeown BA. Functional Morphology of the Teleost
589 Pituitary Gland. American Zoologist. 2015;13(3):719-42.
590 13. Honji RM, Nóbrega RH, Pandolfi M, Shimizu A, Borella MI, Moreira RG.
591 Immunohistochemical study of pituitary cells in wild and captive Salminus hilarii (Characiformes:
592 Characidae) females during the annual reproductive cycle. SpringerPlus. 2013;2(1):460.
593 14. Aoki K, Umeura H. Cell Types in the Pituitary of the Medaka (Oryzias latipes).
594 Endocrinologia Japonica. 1970;17(1):45-55.
595 15. Mukai T, Oota Y. Histological Changes in the Pituitary, Thyroid Gland and Gonads of the
596 Fourspine Sculpin (Cottus kazika) during Downstream Migration. Zoological Science.
597 1995;12(1):91-7.
598 16. Camacho LR, Pozzi AG, de Freitas EG, Shimizu A, Pandolfi M. Morphological and
599 immunohistochemical comparison of the pituitary gland between a tropical Paracheirodon
600 axelrodi and a subtropical Aphyocharax anisitsi characids (Characiformes: Characidae) %J
601 Neotropical Ichthyology. 2020;18.
602 17. Sánchez Cala F, Portillo A, Martín del Río MP, Mancera JM. Immunocytochemical
603 characterization of adenohypophyseal cells in the greater weever fish (Trachinus draco). Tissue
604 and Cell. 2003;35(3):169-78.
605 18. Segura-Noguera MM, Laíz-Carrión R, Martín del Río MP, Mancera JM. An
606 Immunocytochemical Study of the Pituitary Gland of the White Seabream (Diplodus Sargus). The
607 Histochemical Journal. 2000;32(12):733-42.
608 19. Pandolfi M, Cánepa MM, Meijide FJ, Alonso F, Vázquez GR, Maggese MC, et al. Studies on
609 the reproductive and developmental biology of Cichlasoma dimerus (Percifomes, Cichlidae).
610 Biocell. 2009;33(1):1-18.
611 20. Weltzien F-A, Norberg B, Helvik JV, Andersen Ø, Swanson P, Andersson E. Identification
612 and localization of eight distinct hormone-producing cell types in the pituitary of male Atlantic
613 halibut (Hippoglossus hippoglossus L.). Comparative Biochemistry and Physiology Part A:
614 Molecular & Integrative Physiology. 2003;134(2):315-27.
615 21. Kasper RS, Shved N, Takahashi A, Reinecke M, Eppler E. A systematic
616 immunohistochemical survey of the distribution patterns of GH, prolactin, somatolactin, β–TSH,
617 β–FSH, β–LH, ACTH, and α–MSH in the adenohypophysis of Oreochromis niloticus, the Nile tilapia.
618 Cell and Tissue Research. 2006;325(2):303-13.
619 22. Parhar IS, Nagahama Y, Grau EG, Ross RM. Immunocytochemical and Ultrastructural
620 Identification of Pituitary Cell Types in the Protogynous Thalassoma
621 duperrey during Adult Sexual Ontogeny. 1998;15 %J Zoological Science(2):263-76, 14.
622 23. Childs GV. Development of gonadotropes may involve cyclic transdifferentiation of
623 growth hormone cells. Archives of physiology and biochemistry. 2002;110(1-2):42-9.

624 24. Childs GV. Multipotential pituitary cells that contain adrenocorticotropin (ACTH) and
625 other pituitary hormones. Trends in Endocrinology & Metabolism. 1991;2(3):112-7.
626 25. Frawley LS, Boockfor FR. Mammosomatotropes: Presence and Functions in Normal and
627 Neoplastic Pituitary Tissue. Endocrine Reviews. 1991;12(4):337-55.
628 26. Fukami K, Tasaka K, Mizuki J, Kasahara K, Masumoto N, Miyake A, et al. Bihormonal Cells
629 Secreting Both Prolactin and Gonadotropins in Normal Rat Pituitary Cells. Endocrine Journal.
630 1997;44(6):819-26.
631 27. Ben-Shlomo A, Melmed S. Chapter 2 - Hypothalamic Regulation of Anterior Pituitary
632 Function. In: Melmed S, editor. The Pituitary (Third Edition). San Diego: Academic Press; 2011. p.
633 21-45.
634 28. Fontaine R, Ciani E, Haug TM, Hodne K, Ager-Wick E, Baker DM, et al. Gonadotrope
635 plasticity at cellular, population and structural levels: A comparison between fishes and
636 mammals. General and Comparative Endocrinology. 2020;287:113344.
637 29. Wittbrodt J, Shima A, Schartl M. Medaka — a model organism from the far east. Nature
638 Reviews Genetics. 2002;3(1):53-64.
639 30. Naruse K. Genetics, Genomics, and Biological Resources in the Medaka, Oryzias latipes. In:
640 Naruse K, Tanaka M, Takeda H, editors. Medaka: A Model for Organogenesis, Human Disease, and
641 Evolution. Tokyo: Springer Japan; 2011. p. 19-37.
642 31. Siddique K, Ager-Wick E, Fontaine R, Weltzien F-A, Henkel CV. Characterization of
643 hormone-producing cell types in the medaka pituitary gland using single-cell RNA-seq. bioRxiv.
644 2020.
645 32. Kenji Murata, Masato Kinoshita, Kiyoshi Naruse, Minoru Tanaka, Kamei Y. Looking at
646 Adult Medaka. In: Kenji Murata, Masato Kinoshita, Kiyoshi Naruse, Minoru Tanaka, Kamei Y,
647 editors. Medaka: Biology, Management, and Experimental Protocols. 2: John Wiley & Sons; 2019.
648 p. 49-95.
649 33. Burow S, Fontaine R, von Krogh K, Mayer I, Nourizadeh-Lillabadi R, Hollander-Cohen L, et
650 al. Medaka follicle-stimulating hormone (Fsh) and luteinizing hormone (Lh): Developmental
651 profiles of pituitary protein and gene expression levels. General and Comparative Endocrinology.
652 2019;272:93-108.
653 34. Fontaine R, Affaticati P, Yamamoto K, Jolly C, Bureau C, Baloche S, et al. Dopamine Inhibits
654 Reproduction in Female Zebrafish (Danio rerio) via Three Pituitary D2 Receptor Subtypes.
655 Endocrinology. 2013;154(2):807-18.
656 35. Fontaine R, Weltzien F-A. Labeling of Blood Vessels in the Teleost Brain and Pituitary
657 Using Cardiac Perfusion with a DiI-fixative. Journal of Visualized Experiments. 2019(148):e59768.
658 36. Bjerke IE, Øvsthus M, Papp EA, Yates SC, Silvestri L, Fiorilli J, et al. Data integration
659 through brain atlasing: Human Brain Project tools and strategies. European Psychiatry.
660 2018;50:70-6.
661 37. Yates SC, Groeneboom NE, Coello C, Lichtenthaler SF, Kuhn P-H, Demuth H-U, et al.
662 QUINT: Workflow for Quantification and Spatial Analysis of Features in Histological Images From
663 Rodent Brain. Frontiers in Neuroinformatics. 2019;13(75).
664 38. Chapman SC, Sawitzke AL, Campbell DS, Schoenwolf GC. A three-dimensional atlas of
665 pituitary gland development in the zebrafish. Journal of Comparative Neurology.
666 2005;487(4):428-40.
667 39. Farbridge KJ, McDonald-Jones G, McLean CL, Lowry PJ, Etches RJ, Leatherland JF. The
668 development of monoclonal antibodies against salmon (Oncorhynchus kisutch and O. keta)
669 pituitary hormones and their immunohistochemical identification. General and Comparative
670 Endocrinology. 1990;79(3):361-74.
671 40. Naito N, Takahashi A, Nakai Y, Kawauchi H, Hirano T. Immunocytochemical identification
672 of the prolactin-secreting cells in the teleost pituitary with an antiserum to chum salmon
673 prolactin. General and Comparative Endocrinology. 1983;50(2):282-91.

674 41. Wagner GF, McKeown BA. The immunocytochemical localization of pituitary somatotrops
675 in the genus Oncorhynchus using an antiserum to growth hormone of chum salmon
676 (Oncorhynchus keta). Cell Tissue Res. 1983;231(3):693-7.
677 42. Cambré ML, Verdonck W, Ollevier F, Vandesande F, Batten TFC, Kühn ER.
678 Immunocytochemical identification and localization of the different cell types in the pituitary of
679 the seabass (Dicentrarchus labrax). General and Comparative Endocrinology. 1986;61(3):368-75.
680 43. Quesada J, Lozano MT, Ortega A, Agulleiro B. Immunocytochemical and ultrastructural
681 characterization of the cell types in the adenohypophysis of Sparus aurata L. (Teleost). General
682 and Comparative Endocrinology. 1988;72(2):209-25.
683 44. Toubeau G, Poilve A, Baras E, Nonclercq D, De Moor S, Beckers JF, et al.
684 Immunocytochemical study of cell type distribution in the pituitary of Barbus barbus (Teleostei,
685 Cyprinidae). General and Comparative Endocrinology. 1991;83(1):35-47.
686 45. Huang L, Specker JL. Growth Hormone- and Prolactin-Producing Cells in the Pituitary
687 Gland of Striped Bass (Morone saxatilis): Immunocytochemical Characterization at Different Life
688 Stages. General and Comparative Endocrinology. 1994;94(2):225-36.
689 46. Borella MI, Venturieri R, Mancera JM. Immunocytochemical identification of
690 adenohypophyseal cells in the pirarucu (Arapaima gigas), an Amazonian basal teleost. Fish
691 Physiology and Biochemistry. 2009;35(1):3-16.
692 47. Olivereau M, Nagahama Y. Immunocytochemistry of gonadotropic cells in the pituitary of
693 some teleost species. General and Comparative Endocrinology. 1983;50(2):252-60.
694 48. Dubourg P, Burzawa-Gerard E, Chambolle P, Kah O. Light and electron microscopic
695 identification of gonadotrophic cells in the pituitary gland of the goldfish by means of
696 immunocytochemistry. General and Comparative Endocrinology. 1985;59(3):472-81.
697 49. Nozaki M, Naito N, Swanson P, Miyata K, Nakai Y, Oota Y, et al. Salmonid pituitary
698 gonadotrophs I. Distinct cellular distributions of two gonadotropins, GTH I and GTH II. General
699 and Comparative Endocrinology. 1990;77(3):348-57.
700 50. Grandi G, Colombo G, Chicca M. Immunocytochemical studies on the pituitary gland of
701 Anguilla anguilla L., in relation to early growth stages and diet-induced sex differentiation.
702 General and Comparative Endocrinology. 2003;131(1):66-76.
703 51. García-Hernández MP, García-Ayala A, Elbal MT, Agulleiro B. The adenohypophysis of
704 Mediterranean yellowtail, Seriola dumerilii (Risso, 1810): an immunocytochemical study. Tissue
705 and Cell. 1996;28(5):577-85.
706 52. Grandi G, Chicca M. Early development of the pituitary gland in Acipenser naccarii
707 (Chondrostei, Acipenseriformes): an immunocytochemical study. Anatomy and Embryology.
708 2004;208(4):311-21.
709 53. Batten TFC. Immunocytochemical demonstration of pituitary cell types in the teleost
710 Poecilia latipinna, by light and electron microscopy. General and Comparative Endocrinology.
711 1986;63(1):139-54.
712 54. Gutnick A, Blechman J, Kaslin J, Herwig L, Belting H-G, Affolter M, et al. The Hypothalamic
713 Neuropeptide Oxytocin Is Required for Formation of the Neurovascular Interface of the Pituitary.
714 Developmental Cell. 2011;21(4):642-54.
715 55. Golan M, Zelinger E, Zohar Y, Levavi-Sivan B. Architecture of GnRH-Gonadotrope-
716 Vasculature Reveals a Dual Mode of Gonadotropin Regulation in Fish. Endocrinology.
717 2015;156(11):4163-73.
718 56. Kawabata-Sakata Y, Nishiike Y, Fleming T, Kikuchi Y, Okubo K. Androgen-dependent sexual
719 dimorphism in pituitary tryptophan hydroxylase expression: relevance to sex differences in
720 pituitary hormones. Proceedings of the Royal Society B: Biological Sciences.
721 2020;287(1928):20200713.
722 57. Taranger GL, Carrillo M, Schulz RW, Fontaine P, Zanuy S, Felip A, et al. Control of puberty
723 in farmed fish. General and Comparative Endocrinology. 2010;165(3):483-515.

58. Borg B. Androgens in teleost fishes. Comparative Biochemistry and Physiology Part C: Pharmacology, Toxicology and Endocrinology. 1994;109(3):219-45.
59. Royan MR, Kanda S, Kayo D, Song W, Ge W, Weltzien F-A, et al. Gonadectomy and Blood Sampling Procedures in the Small Size Teleost Model Japanese Medaka (Oryzias latipes). JoVE. 2020(166):e62006.
60. Ohta K, Mine T, Yamaguchi A, Matsuyama M. Sexually dimorphic expression of pituitary glycoprotein hormones in a sex-changing fish (Pseudolabrus sieboldi). Journal of Experimental Zoology Part A: Ecological Genetics and Physiology. 2008;309A(9):534-41.
61. Martin SAM, Wallner W, Youngson AF, Smith T. Differential expression of Atlantic salmon thyrotropin β subunit mRNA and its cDNA sequence. Journal of Fish Biology. 1999;54(4):757-66.
62. He W, Dai X, Chen X, He J, Yin Z. Zebrafish pituitary gene expression before and after sexual maturation. Journal of Endocrinology. 2014;221(3):429.
63. Fontaine R, Ager-Wick E, Hodne K, Weltzien F-A. Plasticity of Lh cells caused by cell proliferation and recruitment of existing cells. Journal of Endocrinology. 2019;240(2):361.
64. Rand-Weaver M, Swanson P, Kawauchi H, Dickhoff WW. Somatolactin, a novel pituitary protein: purification and plasma levels during reproductive maturation of coho salmon. Journal of Endocrinology. 1992;133(3):393.
65. Mousa MA, Mousa SA. Immunocytochemical Study on the Localization and Distribution of the Somatolactin Cells in the Pituitary Gland and the Brain ofOreochromis niloticus(Teleostei, Cichlidae). General and Comparative Endocrinology. 1999;113(2):197-211.
66. Mousa MA, Mousa SA. Implication of somatolactin in the regulation of sexual maturation and spawning of Mugil cephalus. Journal of Experimental Zoology. 2000;287(1):62-73.
67. Benedet S, Björnsson BT, Taranger GL, Andersson E. Cloning of somatolactin alpha, beta forms and the somatolactin receptor in Atlantic salmon: seasonal expression profile in pituitary and ovary of maturing female broodstock. Reproductive biology and endocrinology. 2008;6:42-.
68. Onuma T, Kitahashi T, Taniyama S, Saito D, Ando H, Urano A. Changes in expression of genes encoding gonadotropin subunits and growth hormone/prolactin/somatolactin family hormones during final maturation and freshwater adaptation in prespawning chum salmon. Endocrine. 2003;20(1):23-33.
69. Fontaine R, Royan MR, von Krogh K, Weltzien F-A, Baker DM. Direct and Indirect Effects of Sex Steroids on Gonadotrope Cell Plasticity in the Teleost Fish Pituitary. Frontiers in Endocrinology. 2020;11(858).
70. Childs GV, MacNicol AM, MacNicol MC. Molecular Mechanisms of Pituitary Cell Plasticity. Frontiers in Endocrinology. 2020;11(656).
71. Rizzoti K. Adult pituitary progenitors/stem cells: from in vitro characterization to in vivo function. 2010;32(12):2053-62.
72. Ho Y, Hu P, Peel MT, Chen S, Camara PG, Epstein DJ, et al. Single-cell transcriptomic analysis of adult mouse pituitary reveals sexual dimorphism and physiologic demand-induced cellular plasticity. Protein & Cell. 2020;11(8):565-83.
73. Fabian P, Tseng KC, Smeeton J, Lancman JJ, Dong PDS, Cerny R, et al. Lineage analysis reveals an endodermal contribution to the vertebrate pituitary. Science. 2020;370(6515):463-7.
74. Batten T, Ball JN, Benjamin M. Ultrastructure of the adenohypophysis in the teleost Poecilia latipinna. Cell and Tissue Research. 1975;161(2):239-61.
75. Margolis-Kazan H, Peute J, Schreibman MP, Halpern LR. Ultrastructural localization of gonadotropin and luteinizing hormone releasing hormone in the pituitary gland of a teleost fish (the platyfish). Journal of Experimental Zoology. 1981;215(1):99-102.
76. Yan HY, Thomas P. Histochemical and immunocytochemical identification of the pituitary cell types in three sciaenid fishes: Atlantic croaker (Micropogonias undulatus), spotted seatrout (Cynoscion nebulosus), and red drum (Sciaenops ocellatus). General and Comparative Endocrinology. 1991;84(3):389-400.

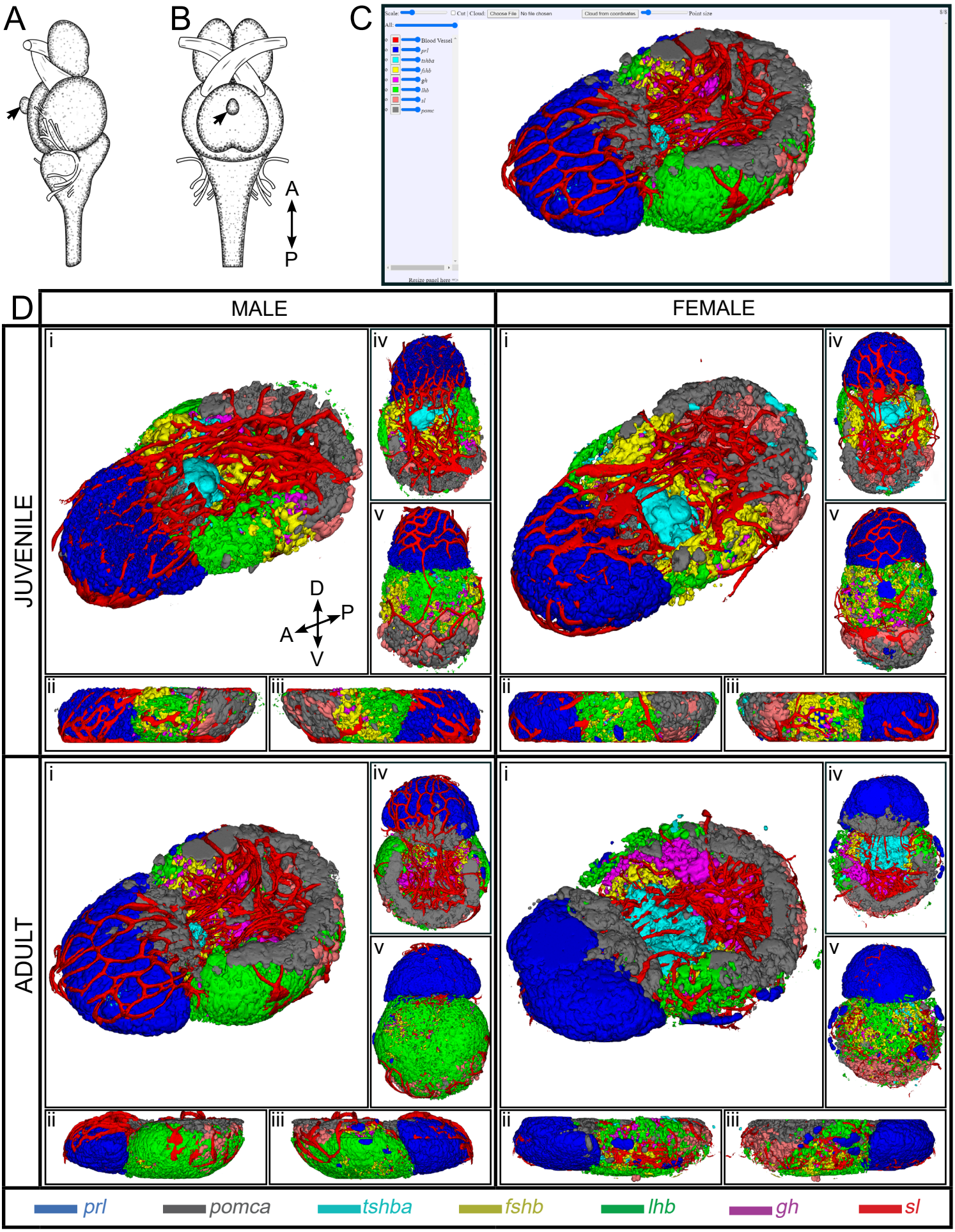

FIGURE 1

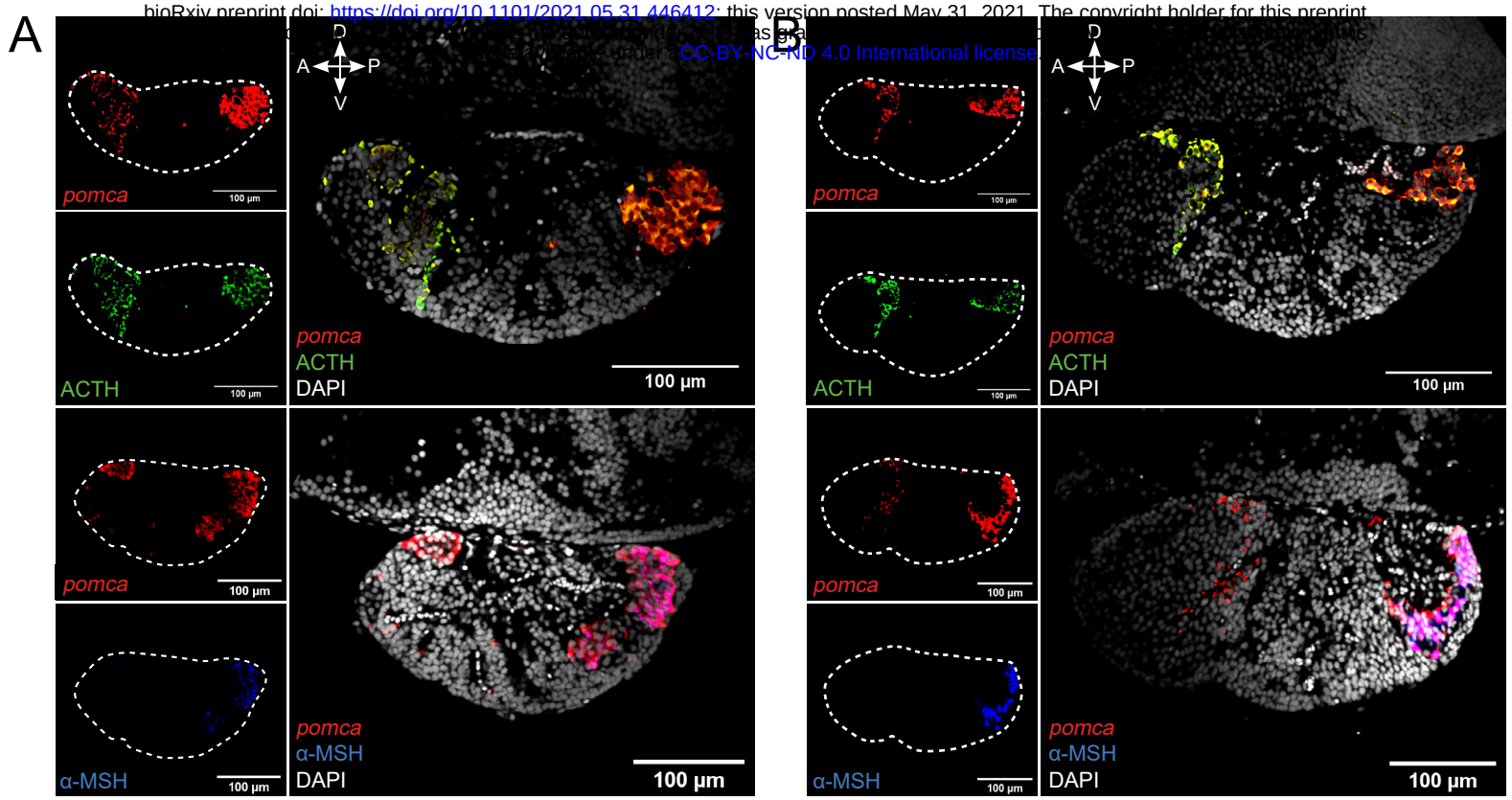

FIGURE 2

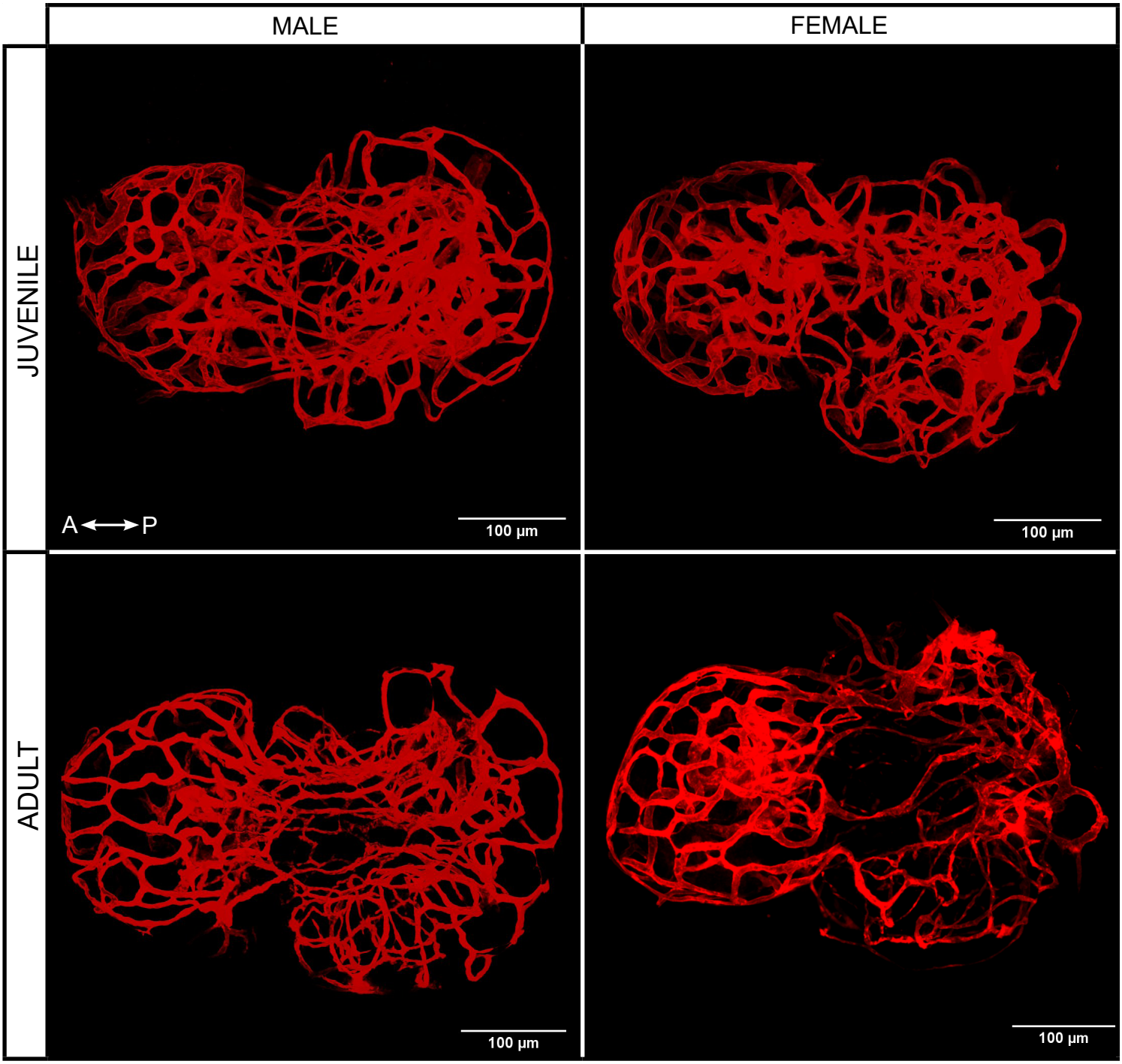

FIGURE 3

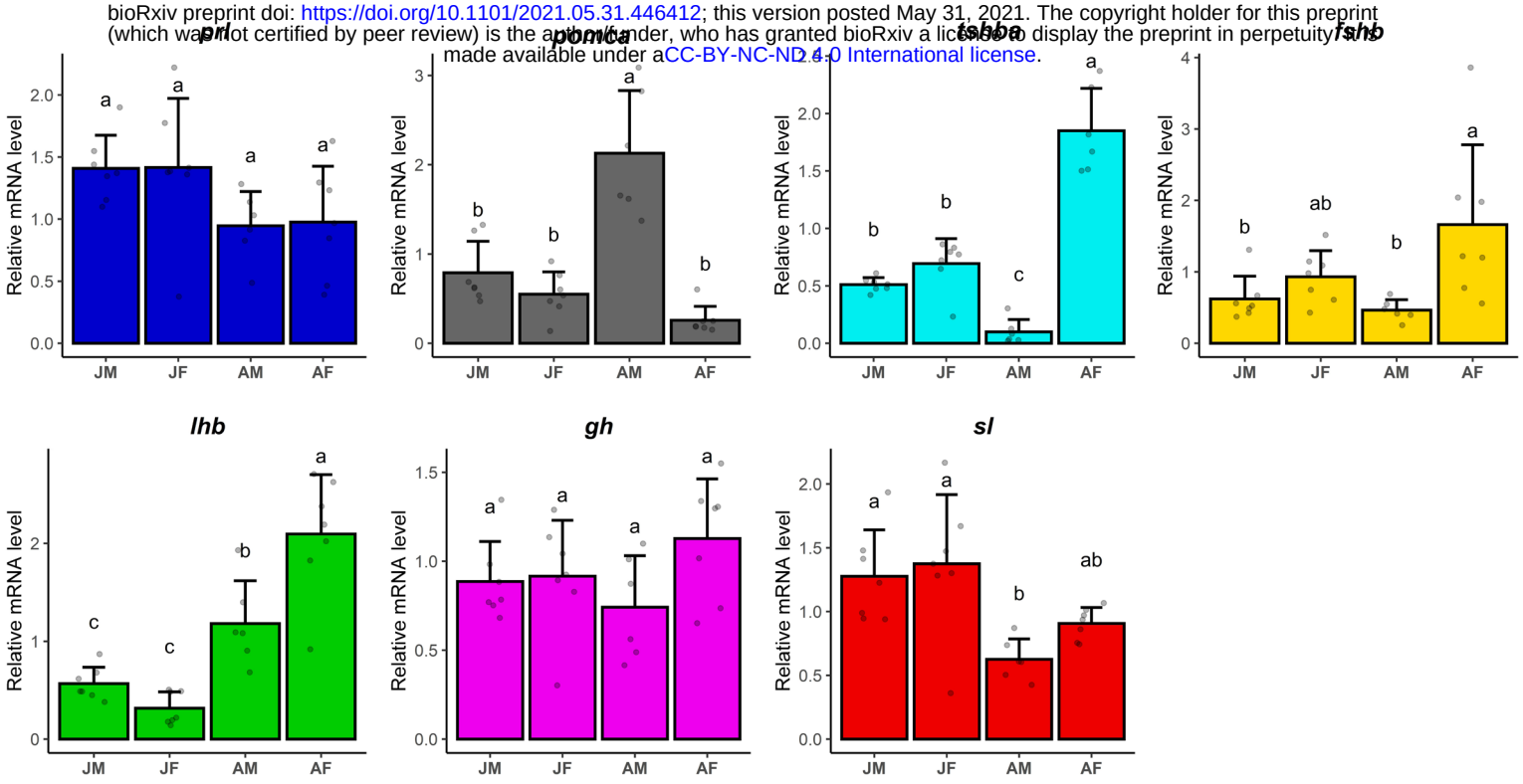

FIGURE 4

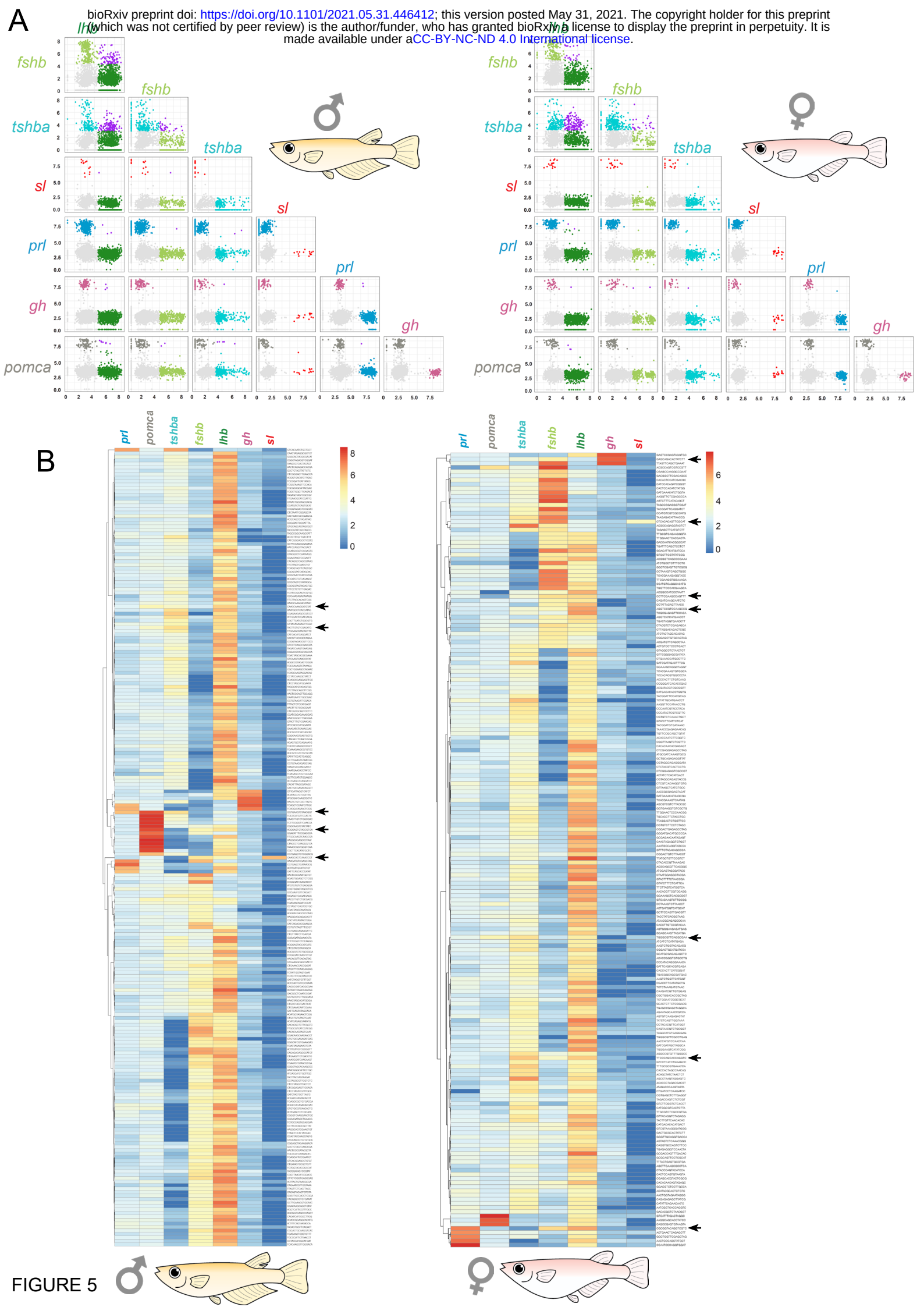

FIGURE 5

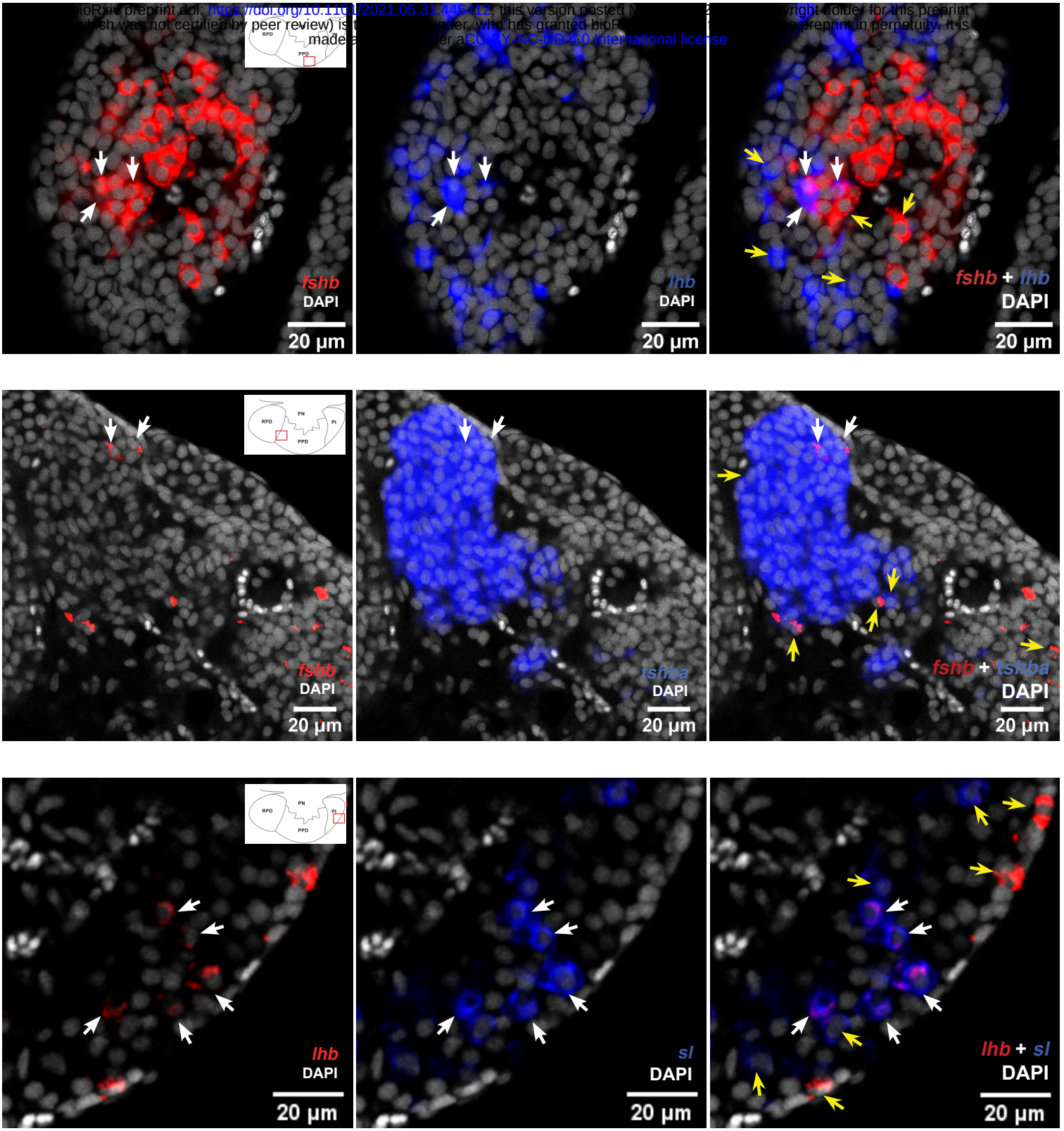

FIGURE 6

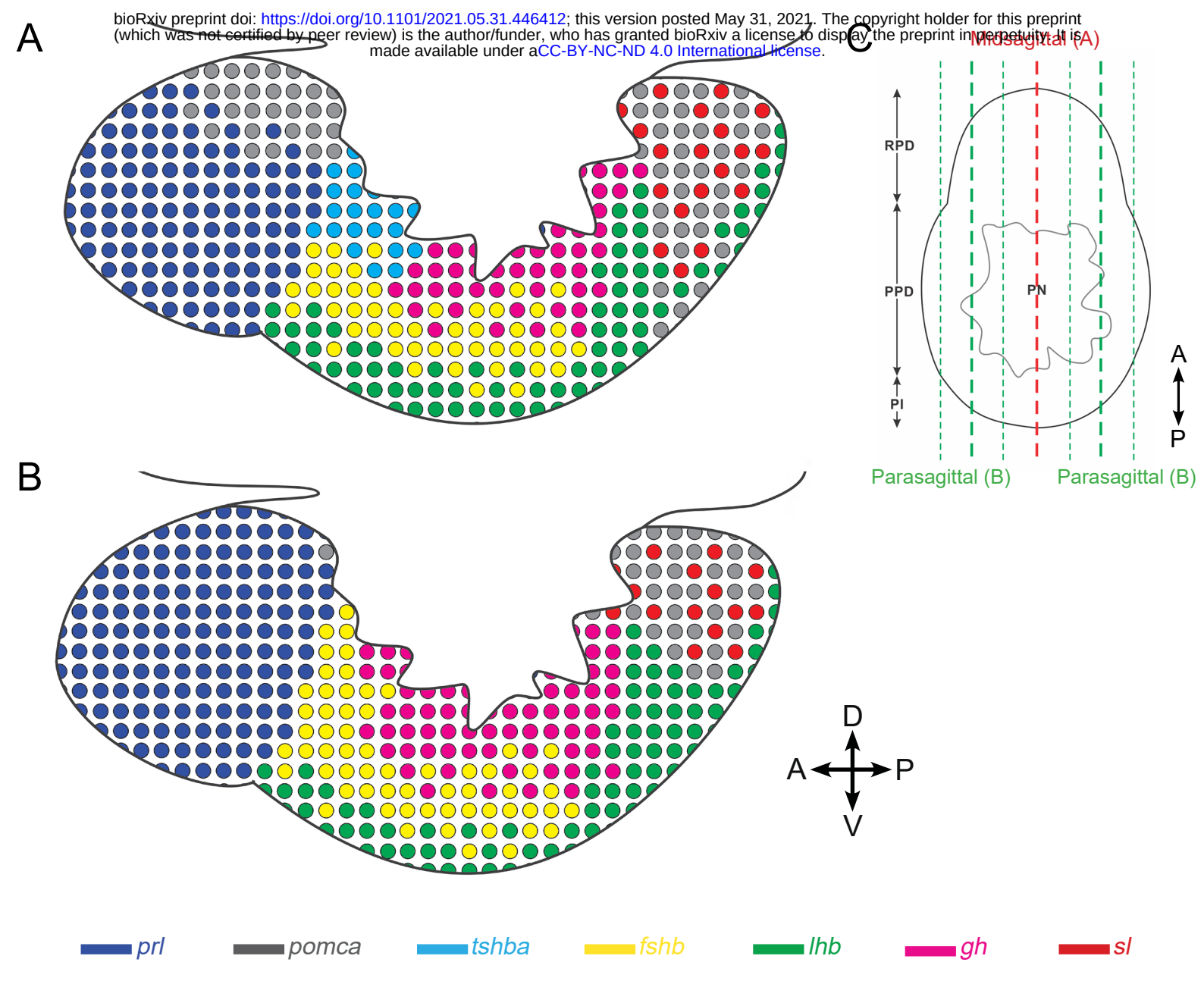

FIGURE 7

Gene Name	Sequence (5' - 3')	Ensembl Gene Name	Accession Number (NCBI/Ensembl)	Amplicon size (bp)	Efficiency	Reference
rpl7	F: TGCTTTGGTGGAGAAAGCTC	*rpl7*	NM_001104870	98	2.03	(Burow et al., 2019)
	R: TGGCAGGCTTGAAGTTCTTT		ENSORLG00000007967			
prl	F: TCAGATGGGAACCAGAGGAC	*prl1*	XM_004071867.4	85	1.987	This study
	R: GATGTCCACGGCTTTACACA		ENSORLG00000016928			
tshba	F: ATGTGGAGAAGCCAGAATGC	*tshba*	XM_004068796.4	88	2	This study
	R: CTCATGTTGCTGTCCCTTGA		ENSORLG00000029251			
lhb	F: CCACTGCCTTACCAAGGACC	*lhb*	NM_001137653.2	100	2	(Hildahl et al., 2012)
	R: AGGAAGCTCAAATGTCTTGTAG		ENSORLG00000003553			
fshb	F: GACGGTGCTACCATGAGGAT	*fshb*	NM_001309017.1	73	2.03	(Burow et al., 2019)
	R: TCCCCACTGCAGATCTTTTC		ENSORLG00000029237			
gh	F: TCGCTCTTTGTCTGGGAGTT	*gh1*	XM_004084500.3	102	1.94	This study
	R: ACATTCTGATTGGCCCTGAT		ENSORLG00000019556			
pomca	F: GTGGTGGTTGTCGGTGGG	*pomca*	XM_004066456.3	122	1.956	This study
	R: GTGAGGTCAGAGCGGCAG		ENSORLG00000025908			
sl	F: CACCAAAGCATTACCCATCC	*smtla*	NM_001104790.1	87	1.965	This study
	R: ACCAGCATCAGCACAGAATG		ENSORLG00000013460			

TABLE 1

Gene	Sequence (5' - 3')	Ensmbl gene name	Accession Number (NCBI/Ensembl)	PCR product size (bp)	Reference
lhb	F: CACAGCCTGCAGATACATGAG	*lhb*	NM_001137653.2	318	Hildahl et al. (2012)
	R: AGGAAGCTCAAATGTCTTGTAG		ENSORLG00000003553		
fshb	F: GAGGAAGCAACACTTTCAGC	*fshb*	NM_001309017.1	500	Hodne et al (2019)
	R: GCACAGTTTCTTTATTTCAGTGC		ENSORLG00000029237		
pomca	F: ATGTATACCGTTTGGTTGCT	*pomca*	XM_004066456.3	515	This study
	R: AAATGCTTCATCTTGTAGGAG		ENSORLG00000025908		
sl	F: CCCATCTTTTCACTGTAAGT	*smtla*	NM_001104790.1	506	This study
	R: ATACTGGAAGGCACCTTGTT		ENSORLG00000013460		
prl	F: GAAAGACCGAGGAGGAACTG	*prl1*	XM_004071867.4	381	This study
	R: TTGCAGAGTTGGACAGGACC		ENSORLG00000016928		
gh	F: TCTCTGCAGACTGAGGAACA	*gh1*	XM_004084500.3	501	This study
	R: AGCCACAGTCAGGTAGGTCT		ENSORLG00000019556		
tshba	F: ACAGGCTAAACTCAAGTTAA	*tshba*	XM_004068796.4	473	This study
	R: AGGATCATATAGGTGCTCTG		ENSORLG00000029251		

TABLE 2

Antibody	Dilution	Source	Reference
Rabbit anti-human ACTH antibody	1:1000	abcam (ab74976)	(Romanò et al., 2017)
Rabbit anti-human α-MSH antibody	1:3000	abcam (ab123811)	(Pravdivyi et al., 2015)
Goat anti-rabbit antibody (Alexa-555)	1:500	Invitrogen (A21429)	(Hodne et al., 2019)

TABLE 3